

Population of high-spin states in ^{23}Na through the $^{11}\text{B}(^{16}\text{O}, \alpha)$ reaction

J. Gomez del Campo*

Instituto de Fisica, Universidad de Mexico, Mexico 20 D. F., Mexico

D. E. Gustafson†

Department of Physics, University of Virginia, Charlottesville, Virginia 22901

R. L. Robinson, P. H. Stelson, P. D. Miller, J. K. Bair, and J. B. McGrory

Oak Ridge National Laboratory, † Oak Ridge, Tennessee 37830

(Received 24 February 1975)

States in ^{23}Na were populated with the $^{11}\text{B}(^{16}\text{O}, \alpha)$ reaction. Energy-averaged differential cross sections were measured in the energy range $E_{c.m.} = 16.9\text{--}18.5$ MeV for 29 excited states in ^{23}Na from 0 to 15 MeV of excitation, and for the laboratory angles of 7, 15, 25, and 150°. Single energy differential cross sections were measured for laboratory angles of 40, 55, and 70° at a bombarding energy of 43.2 MeV. The experimental angular distributions were compared with Hauser-Feshbach calculations, and good agreement was found for the states of known spin values in ^{23}Na . Candidates for high-spin states in ^{23}Na were selected for the ground-state rotational band, and for the $K = \frac{1}{2}^+$ and $K = \frac{1}{2}^-$ bands. The reliability of using Hauser-Feshbach calculations for spin assignments is discussed, and a comparison of the suggested excitation energies for high-spin states with shell-model calculations is presented.

NUCLEAR REACTION $^{11}\text{B}(^{16}\text{O}, \alpha)$, $E_{^{16}\text{O}} = 41.6$ to 45.4 MeV, measured $\sigma(E)$ for $\theta_{\text{lab}} = 7, 15, 25, \text{ and } 150^\circ$; $E_{^{16}\text{O}} = 43.2$ MeV, measured $\sigma(\theta)$; ^{23}Na deduced levels. Hauser-Feshbach calculations and suggested J values. Enriched targets.

I. INTRODUCTION

Heavy ions have permitted exploration of previously inaccessible high-spin states. These investigations have also provided insight into the reaction mechanism associated with heavy-ion induced reactions. Specifically, studies of the reactions $^{10}\text{B}(^{16}\text{O}, \alpha)$ (Ref. 1), $^{12}\text{C}(^{14}\text{N}, ^6\text{Li})$ (Ref. 2), $^{12}\text{C}(^{14}\text{N}, d)$ (Ref. 3), $^{12}\text{C}(^{16}\text{O}, \alpha)$ (Ref. 4), and $^{10}\text{B}(^{16}\text{O}, ^6\text{Li})$ (Ref. 5) have given enough evidence to support a statistical compound-nucleus description for the reaction mechanism, as has been demonstrated by comparing theoretical predictions to cross sections obtained for states of known spin.^{1, 3, 5} The general features of these reactions are explained by Hauser-Feshbach (HF) calculations.⁶

Comparison of the HF predictions with experiment has then been used to determine spins of high-spin states which are selectively excited in these heavy-ion induced reactions.¹ The general conclusion of this work is that one can use statistical-model calculations to predict spin values within one unit of angular momentum, provided that one has a good measurement of the energy-averaged cross sections. However, there are some exceptions to this general trend, particularly for the $^{12}\text{C}(^{16}\text{O}, \alpha)$ reaction reported by Fifield, Zurmühle, and Balamuth.⁷

The known level properties of the low-lying states in ^{23}Na determined through light-ion reac-

tions have been summarized by Endt and Van der Leun.⁸ From the $^{12}\text{C}(^{12}\text{C}, p)$ reaction^{9, 10} some suggestions have been made for high-spin states of the $K = \frac{3}{2}^+$, $K = \frac{1}{2}^+$, and $K = \frac{1}{2}^-$ rotational bands.

In the present study we have measured energy-averaged angular distributions for the $^{11}\text{B}(^{16}\text{O}, \alpha)\text{--}^{23}\text{Na}$ reaction. Comparison of our experimental angular distributions with statistical-model calculations strongly indicates that the statistical compound-nucleus process is the predominant reaction mechanism; the extracted spin values agree with most of the values reported previously,⁸⁻¹⁰ especially for the $K = \frac{3}{2}^+$, $K = \frac{1}{2}^+$, and $K = \frac{1}{2}^-$ rotational bands. We suggest additional high-spin states for these three bands (up to the $\frac{21}{2}^+$, $\frac{17}{2}^+$, and $\frac{15}{2}^-$, respectively). Finally, a comparison between these high-spin states and those predicted by the shell model is presented.

II. EXPERIMENTAL PROCEDURE

Self-supporting, 95% enriched ^{11}B foils with thicknesses of $30 \mu\text{g}/\text{cm}^2$, were bombarded with ^{16}O ions extracted from the Oak Ridge tandem accelerator. The target thicknesses were measured by elastic scattering and α ranging.¹

The reaction α particles were detected with a position-sensitive proportional counter placed at the focal surface of an Enge split-pole magnetic spectrograph. A description of the detector and associated electronics is given elsewhere.⁵

The ^{11}B foils had a small carbon contamination ($\sim 2 \mu\text{g}/\text{cm}^2$). To minimize the potentially severe problem of carbon building up on the target during irradiation a large cold trap was placed between the scattering chamber and diffusion pump. In order to correct the $^{11}\text{B}(^{16}\text{O}, \alpha)$ peaks for carbon contamination, we took a $^{12}\text{C}(^{16}\text{O}, \alpha)$ run after each $^{11}\text{B}(^{16}\text{O}, \alpha)$ run. For all the $^{11}\text{B}(^{16}\text{O}, \alpha)$ peaks that were analyzed, the α particles coming from $^{12}\text{C}(^{16}\text{O}, \alpha)$ amounted to less than 10% of the total area. For some other peaks the carbon contamination contributed as much as 50%. Those cases have not been included in the present analysis. Uncertainties due to the 5% ^{10}B in the target can be neglected since the cross sections for the $^{10}\text{B}(^{16}\text{O}, \alpha)$ measured in Ref. 1 are of almost the same magnitude as the present reaction.

III. RESULTS

Differential cross sections were measured for states excited in ^{23}Na up to 15 MeV. Measurements were made in 400-keV energy intervals from 41.6 to 45.4 MeV for the laboratory angle of 7° , from 41.6 to 44.4 MeV for 15° , from 42.4 to 44.4 MeV for 25° , and from 42.0 to 43.6 MeV for 150° . Single-energy measurements were made at 43.2-MeV bombarding energy for the laboratory angles of 40° , 55° , and 70° . Figure 1 shows a typical spectrum taken at a laboratory energy of 45 MeV and an angle of 7° . The full width at half maximum (FWHM) is of the order of 140 keV and

is due mainly to the target thickness. The strong and selective structure observed is consistent with the population of high-spin states. Also shown in Fig. 1 are some of the states previously reported⁸⁻¹⁰ together with the known members of the ground-state rotational band with spins and energies (MeV), respectively, of $\frac{3}{2}^+$ (0.0), $\frac{5}{2}^+$ (0.439), $\frac{7}{2}^+$ (2.076), $\frac{9}{2}^+$ (2.703), $\frac{11}{2}^+$ (5.536), $\frac{13}{2}^+$ (6.236),^{9, 10} and the suggested $\frac{15}{2}^+$ (9.04)^{9, 10} and $\frac{17}{2}^+$ (9.84).¹⁰ In the present paper we give evidence that the states at 14.24 and 14.70 MeV shown in Fig. 1 are the $\frac{19}{2}^+$ and $\frac{21}{2}^+$ members of the ground-state rotational band.

The peaks labeled C in Fig. 1 correspond to known states in ^{24}Mg excited by the $^{12}\text{C}(^{16}\text{O}, \alpha)$ reaction due to the carbon contaminant in the target. Because of this contamination we lost information for some of the excited states in ^{23}Na . These states were in the energy regions from 7.5 to 8.2, from 9.2 to 9.6, from 10.4 to 10.6, from 11.7 to 13.0, and from 13.3 to 13.5 MeV. As can be seen from Fig. 1 the peak at 9.84 MeV has a width about 50% larger than the one at 11.28 MeV. The broadening of the 9.84-MeV peak can be attributed to contributions of the 9.62-MeV peak partially resolved and a peak due to carbon contamination. For most of the spectra the 9.84-MeV state has a width consistent with the experimental resolution.

The different peaks analyzed were stripped with the light-pen system of a PDP-11 computer with

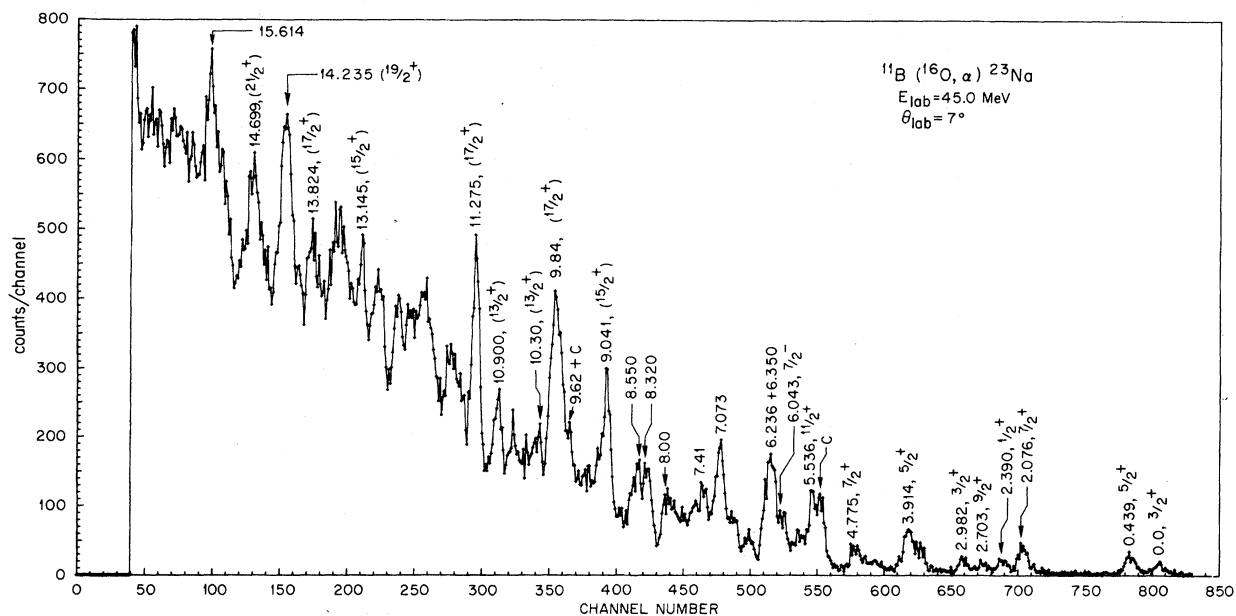


FIG. 1. $^{11}\text{B}(^{16}\text{O}, \alpha)^{23}\text{Na}$ spectrum measured at a bombarding energy of 45 MeV and a laboratory angle of 7° . Peaks labeled C correspond to known states in ^{24}Mg excited by $^{12}\text{C}(^{16}\text{O}, \alpha)$.

a general background subtracted, and an estimate of the tails of any interfering neighboring peaks subtracted. The widths of peaks which were analyzed were all consistent with the experimental resolution of 140–160 keV, which reduces the probability that some of the analyzed peaks were multiplets. Even though most of the evidence indicates that the states reported are single levels one has to recognize that the experimental reso-

lution is perhaps the major source of uncertainty in the present study.

Figure 2 shows our results for some of the excitation functions measured in the energy range from 43.2 to 45.6 MeV. The closed experimental points joined by the solid lines correspond to center-of-mass cross sections measured at a laboratory angle of 7° and the open points joined by the dashed lines correspond to values obtained

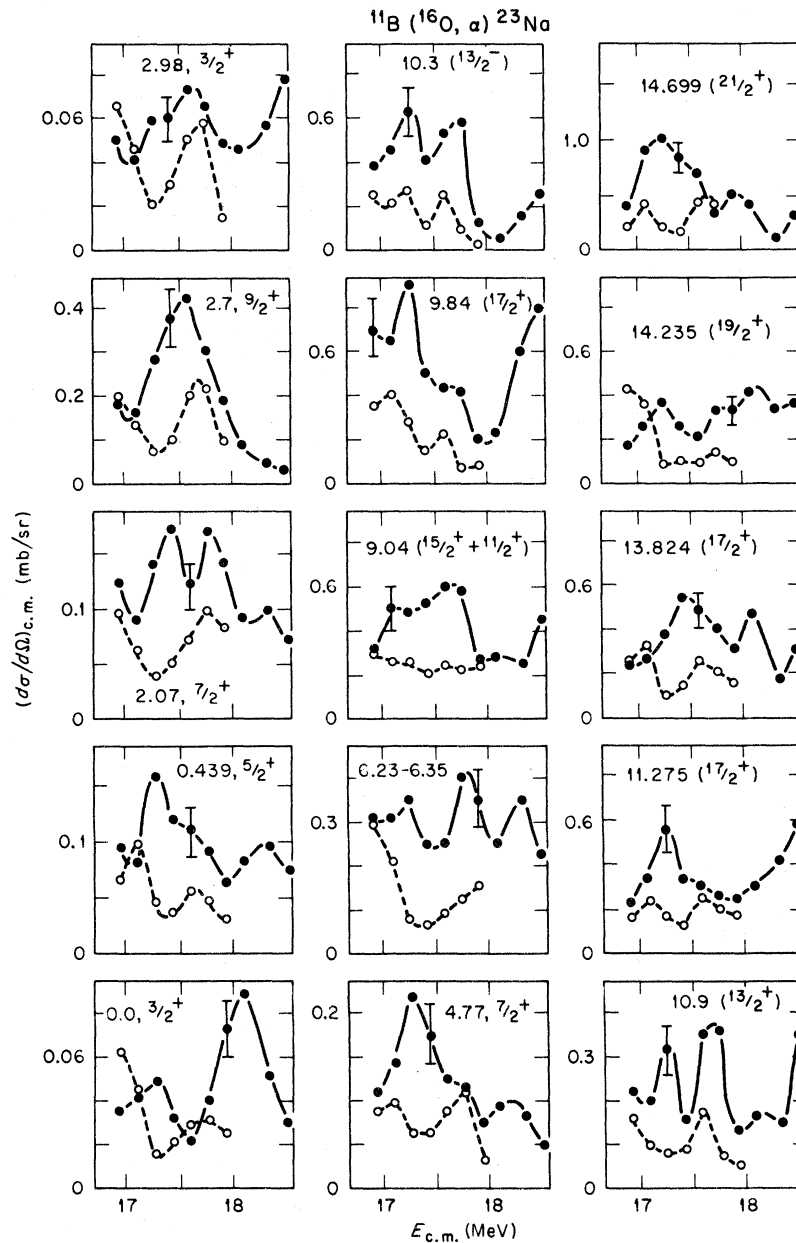


FIG. 2. Excitation functions for some of the excited states in ^{23}Na . The closed experimental points joined by the solid lines correspond to measurements made at a laboratory angle of 7° , and the open points joined by the dashed lines are for a laboratory angle of 15° .

at 15° in the laboratory system. Excitation curves corresponding to 15 states in ^{23}Na , ordered by increasing excitation energy, are shown. The spins and parities indicated are from previous assignments⁸⁻¹⁰ and from the HF predictions discussed in Sec. IV.

The fluctuations of the cross sections observed in Fig. 2 are typical of a compound system that is formed at high excitation energy.¹¹ From the figure one sees that the fluctuations are larger at 7° than at 15° ; this results from the increased number of effective channels at the larger angle.¹² Even though the bombarding energy interval in the present study was too small to permit a meaningful fluctuation analysis, it is about 10 times the coherent width ($\sim 120 \text{ keV}^1$) and this should

certainly be large enough to provide a good estimate of the average cross section.

In order to have differential cross sections averaged at other angles for which the fluctuation phenomena are important, excitation functions were measured at 25° and 150° in the laboratory system. Only single-energy values were measured at laboratory angles of 40° , 55° , and 70° , since for these angles fluctuation effects are expected to be negligible for the case of nonzero entrance- and exit-channel spins.

The 150° cross-section measurements also provided a check on the symmetry of the differential cross sections. However, because of the strong shift in energy of the various α groups with increased angle, the length of the detector allowed

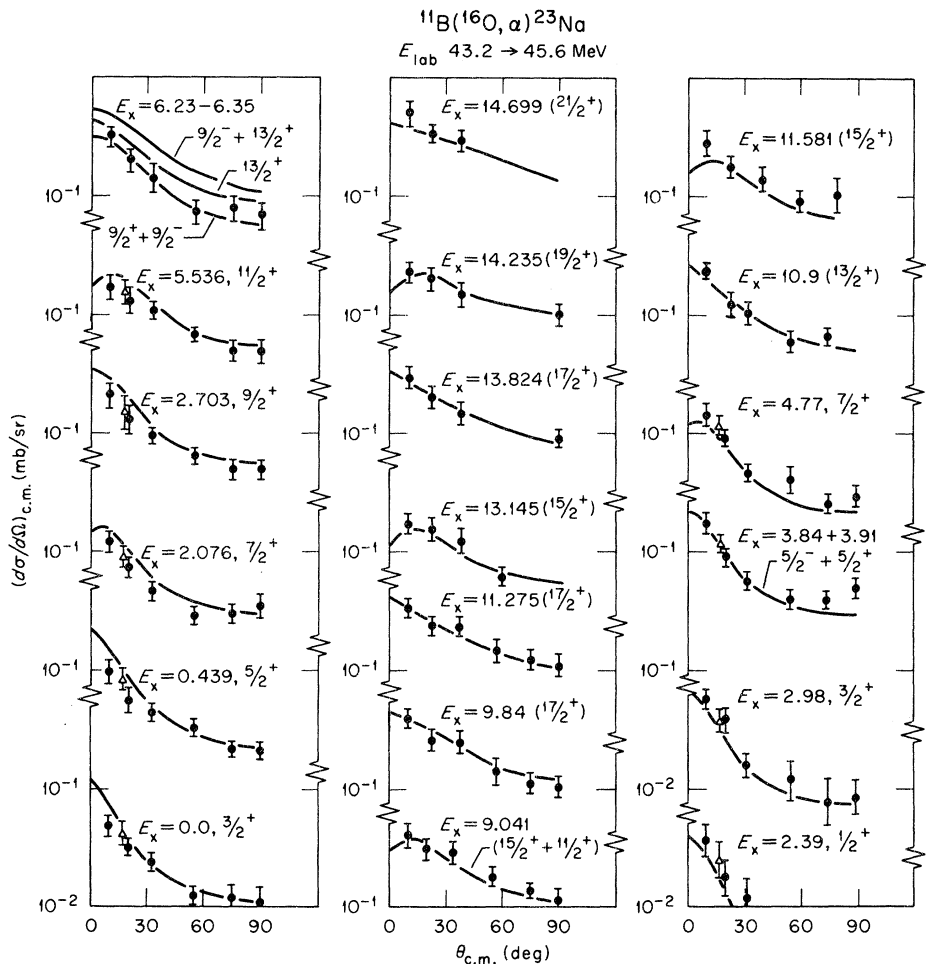


FIG. 3. Angular distributions for some of the excited states in ^{23}Na . The states shown are members of the ground-state rotational band and of the $K = \frac{1}{2}^+$ band together with some other prominent states. The solid dots plotted at c.m. angles of 10° , 22° , and 36° are energy-averaged cross sections, and the ones at c.m. angles of 55° , 75° , and 90° are single energy values obtained at 43.2-MeV bombarding energy. The open triangles are averaged cross sections for a laboratory angle of 150° plotted in the symmetric forward direction. Solid lines are the results of Hauser-Feshbach calculations (see Ref. 6) discussed in Sec. IV of the text.

us to observe states only up to 6 MeV of excitation energy.

The results of our angular distributions are shown in Figs. 3 and 4. For some of the angular distributions the resolution and counting statistics were not good enough to separate the individual states. The experimental points at the c.m. angles of 10, 22, and 36°, represented by the solid circles, are energy-averaged cross sections; the open triangles correspond to the average values at the laboratory angle of 150° plotted in the forward direction, and as can be seen, they are clearly

consistent with symmetry around 90° c.m. The curves drawn through the experimental points in Figs. 3 and 4 are the result of calculations described in Sec. IV.

Table I summarizes our results for the different states analyzed. The first column gives the excitation energy from Ref. 8 except for states higher than 9 MeV which are from this work. Column 2 lists the values of spin and parity reported in Refs. 8-10, column 3 gives the quantum numbers of the rotational bands identified in Ref. 9, and column 4 presents the values for spin-parity sug-

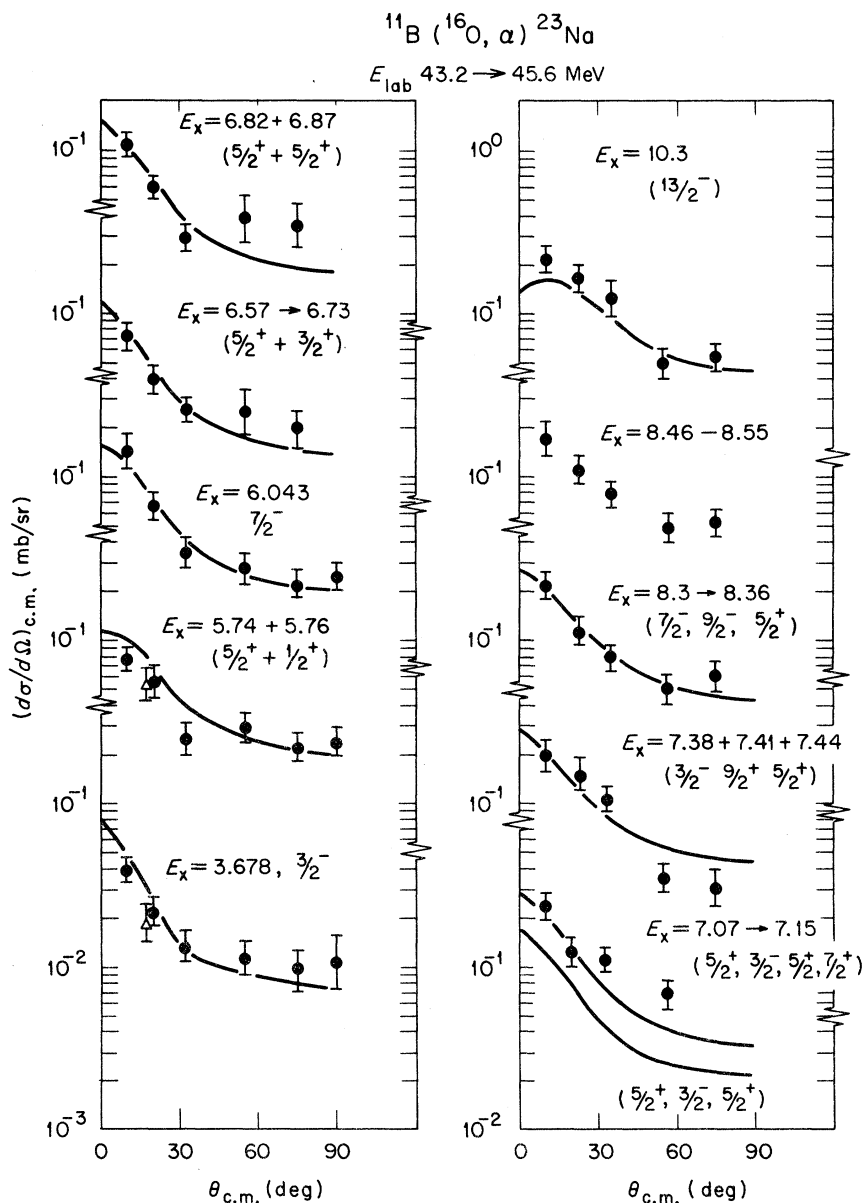


FIG. 4. Angular distributions for some of the excited states in ^{23}Na . Shown are some members of the $K = \frac{1}{2}^-$ band together with some states not resolved. Details are described in the caption of Fig. 3.

TABLE I. Cross sections for the $^{11}\text{B}(^{16}\text{O}, \alpha)^{23}\text{Na}$ reactions. The brackets cover the cross sections to unresolved states.

E_x^a (MeV)	$J^\pi{}^a$	$K^\pi{}^b$	$J^\pi{}^c$	$\langle d\sigma/d\Omega \rangle_{\text{exp}}$ (mb/sr)		
				10° c.m.	22° c.m.	36° c.m.
0.0	$\frac{3}{2}^+$	$\frac{3}{2}^+$	$\frac{3}{2}^+$	0.047	0.032	0.024
0.439	$\frac{5}{2}^+$	$\frac{3}{2}^+$	$\frac{5}{2}^+$	0.097	0.055	0.043
2.076	$\frac{7}{2}^+$	$\frac{3}{2}^+$	$\frac{7}{2}^+$	0.123	0.072	0.046
2.390	$\frac{1}{2}^+$	$\frac{1}{2}^+$	$\frac{1}{2}^+$	0.038	0.017	0.012
2.639	$\frac{1}{2}^-$	$\frac{1}{2}^-$	$\frac{3}{2}^+$	0.21	0.131	0.096
2.703	$\frac{9}{2}^+$	$\frac{3}{2}^+$				
2.982	$\frac{3}{2}^+$	$\frac{1}{2}^+$	$\frac{3}{2}^+$	0.058	0.04	0.016
3.678	$\frac{3}{2}^-$	$\frac{1}{2}^-$	$\frac{3}{2}^-$	0.040	0.023	0.013
3.848	$\frac{5}{2}^-$	$\frac{1}{2}^-$	$\frac{5}{2}^+$	0.178	0.09	0.056
3.914	$\frac{5}{2}^+$	$\frac{1}{2}^+$				
4.432	$\frac{1}{2}^+$					
4.775	$\frac{7}{2}^+$	$\frac{1}{2}^+$	$\frac{7}{2}^+$	0.145	0.09	0.044
5.380	$(\frac{3}{2}, \frac{5}{2})^+$					
5.536	$(\frac{5}{2} \rightarrow \frac{11}{2})$	$(\frac{3}{2})$	$\frac{11}{2}^+$	0.176	0.14	0.101
5.740	$(\frac{3}{2}, \frac{5}{2})^+$		$(\frac{5}{2}^+, \frac{3}{2}^+)$ $(\frac{1}{2}^+, \frac{3}{2}^+)$	0.076	0.054	0.025
5.766						
5.781						
5.931						
5.967	$(\frac{1}{2}, \frac{3}{2})^-$		$\frac{1}{2}^-$	0.131	0.07	0.035
6.043		$(\frac{1}{2}^-)^d$				
6.117						
6.191						
6.236	$(\frac{9}{2}, \frac{13}{2})^+$		$\frac{9}{2}^+, (\frac{13}{2}^+)$	0.321	0.21	0.14
	$\frac{13}{2}^{+b}$	$(\frac{3}{2}^+)$				
6.263	$\frac{1}{2}^+$		$\frac{1}{2}^+$	0.071	0.04	0.025
6.308	$\frac{1}{2}^+$					
6.350	$\frac{9}{2}^- (\frac{7}{2}^-)$	$\frac{1}{2}^-$	$\frac{9}{2}^-$	0.071	0.04	0.025
6.577	$(\frac{5}{2}, \frac{9}{2})$		$\frac{5}{2}^+$			
6.617			$\frac{1}{2}$			
6.734	$(\frac{3}{2}, \frac{5}{2})^+$		$\frac{3}{2}^+$			
6.818			$(\frac{5}{2}^+, \frac{7}{2}^+)$ $(\frac{5}{2}^+, \frac{3}{2}^+)$	0.107	0.06	0.03
6.867	$(\frac{3}{2}, \frac{5}{2})^+$					
6.920	$(\frac{3}{2}^-)$					
6.949						
7.073	$(\frac{5}{2})$		$\frac{5}{2}^+$ $\frac{3}{2}^-$	0.228	0.127	0.11
7.084	$(\frac{3}{2}^-)$					
7.135	$(\frac{3}{2}, \frac{5}{2})^+$		$(\frac{5}{2}^+, \frac{3}{2}^+)$ $(\frac{7}{2}^+, \frac{9}{2}^+)$			
7.156						
7.180						
7.272						

TABLE I (Continued).

E_x^a (MeV)	J^π^a	K^π^b	J^π^c	$\langle d\sigma/d\Omega \rangle_{\text{exp}}$ (mb/sr)		
				10° c.m.	22° c.m.	36° c.m.
7.386	$(\frac{1}{2}^-, \frac{3}{2}^-)$		$(\frac{3}{2}^-, \frac{1}{2}^-)$	0.209	0.164	0.1
7.410		$(\frac{1}{2}^+)^d$	$(\frac{3}{2}^+, \frac{11}{2}^-)$			
7.446	$(\frac{3}{2}^+, \frac{5}{2}^+)$		$(\frac{5}{2}^+, \frac{3}{2}^+)$			
8.299			$(\frac{7}{2}^-, \frac{9}{2}^-)$	0.234	0.103	0.08
8.320			$(\frac{7}{2}^-, \frac{5}{2}^-)$			
8.360			$(\frac{7}{2}^-, \frac{5}{2}^-)$			
8.415						
8.467	$(\frac{3}{2}^+, \frac{5}{2}^+)$			0.180	0.108	0.08
8.498						
8.555						
8.602						
8.94 ^b		$(\frac{1}{2}^+)^d$	$\frac{11}{2}^+$	0.424	0.3	0.29
9.041	$(\frac{15}{2}^+)^{b,e}$	$(\frac{3}{2}^+)^{d,e}$	$\frac{15}{2}^+$			
9.84 ^f	$(\frac{17}{2}^+)^e$	$(\frac{3}{2}^+)^{d,e}$	$\frac{17}{2}^+$	0.400	0.24	0.24
10.3 ^f	$(\frac{13}{2}^-)^b$	$(\frac{1}{2}^-)^b$	$(\frac{13}{2}^+, \frac{13}{2}^-)$	0.222	0.172	0.13
10.9 ^f		$(\frac{1}{2}^+)^d$	$\frac{13}{2}^+$	0.239	0.12	0.1
11.28 ^f			$\frac{17}{2}^+$	0.348	0.24	0.24
11.58 ^f		$(\frac{1}{2}^-)^d$	$(\frac{15}{2}^+, \frac{15}{2}^-)$	0.29	0.173	0.14
13.15 ^f		$(\frac{1}{2}^+)^d$	$(\frac{15}{2}^+, \frac{15}{2}^-)$	0.176	0.168	0.13
13.82 ^f		$(\frac{1}{2}^+)^d$	$\frac{17}{2}^+$	0.300	0.207	0.15
14.24 ^f		$(\frac{3}{2}^+)^d$	$(\frac{19}{2}^+, \frac{17}{2}^+)$	0.25	0.19	0.16
14.7 ^f		$(\frac{3}{2}^+)^d$	$\frac{21}{2}^+$	0.51	0.33	0.30

^a See Ref. 8.^b See Ref. 9.^c Spins suggested by Hauser-Feshbach fits (see Ref. 6) to the angular distributions.^d Suggested by the present experiment.^e See Ref. 10.^f Excitation energies from this experiment. All ± 60 keV.

gested by the HF calculations. Columns 5 to 7 are the energy-averaged differential cross sections for the center-of-mass angles 10°, 22°, and 36°. The absolute errors vary from ± 15 to $\pm 20\%$ depending on target-thickness uncertainty, counting statistics, and background subtraction.

IV. HAUSER-FESHBACH ANALYSIS

A. Dependence of the calculations on optical-model and level density parameters

Average compound-nucleus cross sections were calculated with the familiar HF expressions for total and differential cross sections with the computer code HELGA.¹³ Details of this type of calculations are given elsewhere.^{1, 2, 4, 14}

Table II shows the level density and optical-model parameters used in the calculations for the ten reaction channels which were included. The level density employed is essentially the one given in Ref. 1 which has two independent parameters, the level-density parameter a and the pairing-energy correction Δ . Values for Δ have been taken from the work of Gilbert and Cameron¹⁵ and are shown in the second row of Table II. The values of the level-density parameter a shown in the first row are from Ref. 16 except for the α , β , and n channels whose values are $A/7.5$, $A/8.4$, and $A/7.5$, respectively. With these values we reproduced essentially the absolute cross sections for the 2.703-MeV $\frac{9}{2}^+$ and 9.84-MeV $(\frac{17}{2}^+)$ (Ref. 10) states shown in Fig. 3. The ratio of the total cross

TABLE II. Level density and optical -model parameters for the $^{16}\text{O} + ^{11}\text{B}$ reaction.

	$^{23}\text{Na} + \alpha$	$^{26}\text{Mg} + p$	$^{26}\text{Al} + n$	$^{25}\text{Mg} + d$	$^{24}\text{Mg} + t$	$^{22}\text{Ne} + ^5\text{Li}$	$^{19}\text{F} + ^8\text{Be}$	$^{15}\text{N} + ^{12}\text{C}$	$^{13}\text{C} + ^{14}\text{N}$	$^{11}\text{B} + ^{16}\text{O}$
a	3.06 ^a	3.10 ^a	3.46 ^a	3.70 ^b	3.58 ^b	2.93 ^a				
Δ^c	2.67	4.26	0.0	2.46	5.13	6.0				
E_c (MeV)	14.7	6.9	3.75	4.4	10.0	7.8	6.5	10.1	12.0	13.0
No. of discrete levels	255	20	23	14	28	30	30	20	30	26
V (MeV)	99.9 ^d	56.99 - 0.55E ^e	47.01 - 0.26E ^e	89.3 - 0.22E ^e	166.1 ^f		7.5 + 0.4E _{cm.g}		100.0 ^h	
$R_0 = r_0 A^{1/3}$ fm	4.25 ^d	3.70 ^e	3.86 ^e	3.36 ^c	3.10 ^f		1.35(A ₁ ^{1/3} + A ₂ ^{1/3}) ^g		1.19(A ₁ ^{1/3} + A ₂ ^{1/3}) ^h	
a_0 (fm)	0.60 ^d	0.65 ^e	0.66 ^e	0.81 ^e	0.83 ^f		0.45 ^g		0.48 ^h	
W (MeV)	11.3 ^d	13.50 ^e	9.52 - 0.053E ^e	14.4 + 0.24E ^e	19.30 ^f		0.4 + 0.125E _{cm.g}		28.70 ^h	
$R_f = r_f A^{1/3}$ fm	4.25 ^d	4.29 ^e	3.72 ^e	3.92 ^e	4.98 ^f		1.35(A ₁ ^{1/3} + A ₂ ^{1/3}) ^g		1.26(A ₁ ^{1/3} + A ₂ ^{1/3}) ^h	
a_i (fm)	0.60 ^d	0.47 ^e	0.48 ^e	0.68 ^e	0.87 ^f		0.45 ^g		0.26 ^h	
R_{Coul} (fm)	4.25 ^d	3.70 ^e		3.36 ^e	3.10 ^f		1.35(A ₁ ^{1/3} + A ₂ ^{1/3}) ^g		1.26(A ₁ ^{1/3} + A ₂ ^{1/3}) ^h	

^a Values of a are $A/7.5$ for α and n channels,

$A/8.4$ for p channel and $A/6.4$ for ^5Li channel.

^b Values from Ref. 16.

^c Values from Ref. 15.

^d Values from Ref. 21.

^e Values from Ref. 22.

^f Values from Ref. 23.

^g Values from Ref. 18.

^h Values from Ref. 17.

sections calculated for these two states with the parameters of Table II is $\sigma(\frac{17}{2})/\sigma(\frac{9}{2}) = 2.120$. By varying the level-density parameter a in the p channel to $A/7.5$ we found that the ratio $\sigma(\frac{17}{2})/\sigma(\frac{9}{2})$ was only changed by 3% to 2.059 in the relative total cross sections. However, the absolute value of cross sections was reduced by ~33%.

This variation of the cross sections with level-density parameters is similar to the ones reported by Fifield *et al.*⁷ and illustrates the fact that even though relative cross sections do not change significantly with variations in the parameters, absolute cross sections do. The uncertainty of the absolute values depends mainly on the level density parameters of the various channels whose continuum contribution is predominant.

The quantity E_c listed in the third row of Table II indicates the energy where the discrete spectrum was substituted by the level density. The discrete states included in the Hauser-Feshbach calculations for the different reaction channels are those experimentally established except for the ^{23}Na nucleus where besides the known or previously suggested⁸⁻¹⁰ states we include a number of states needed to match the ones predicted by the level density.

In the preceding discussion it was assumed that the optical-model parameters for entrance and exit channels were fixed. Dependence on these parameters has been given in Ref. 7 for the $^{12}\text{C}-(^{16}\text{O}, \alpha)$ reaction. For the present case we calculated cross sections for two different sets of optical-model parameters in the entrance channel. One set shown in Table II, which fits elastic scattering data¹⁷ and the other proposed by Malmin and used for the other heavy-ion channels.¹⁸ We found up to 25% variation in the absolute scale of the cross sections for all the states analyzed and little variation (<5%) in the relative cross sections.

B. Comparison to experimental data

Figures 3 and 4 show the theoretical and experimental angular distributions and as can be seen the over-all agreement, in shape and magnitude, is quite satisfactory. However, since the absolute Hauser-Feshbach cross sections depend strongly on the level density and optical-model parameters, as discussed previously, the agreement with the experimental data must be understood in the sense that the relative cross sections for the different states populated by the $^{11}\text{B}(^{16}\text{O}, \alpha)$ reaction, are completely consistent with the statistical-model predictions. Figure 3 shows members of the ground-state rotational band whose energies (MeV) and spin-parities are: 0.0, $\frac{3}{2}^+$; 0.439, $\frac{5}{2}^+$; 2.076, $\frac{7}{2}^+$; 2.703, $\frac{9}{2}^+$; and 5.536, $\frac{11}{2}^+$.

Also shown in Fig. 3 are some known members of the $K = \frac{1}{2}^+$ band; these are the 2.39, $\frac{1}{2}^+$; 2.98, $\frac{3}{2}^+$; 3.91, $\frac{5}{2}^+$; and 4.77, $\frac{7}{2}^+$ states. The angular distribution for the 3.91-MeV group was unresolved from the 3.84, $\frac{5}{2}^-$ member of the $K = \frac{1}{2}^-$ band and the Hauser-Feshbach curve corresponds to the $\frac{5}{2}^+$ and $\frac{5}{2}^-$ states. States assigned to the $K = \frac{1}{2}^-$ rotational band are shown in Fig. 4 and their energies (MeV) and spin-parities are 3.68, $\frac{3}{2}^-$; 6.04, $\frac{7}{2}^-$. The $\frac{7}{2}^-$ assignment of the 6.04-MeV state was only suggested by Frank *et al.*,⁹ but our angular distribution supports this assignment.

The excellent agreement between the statistical-model calculations and the experimental results for the states whose spin-parities have been previously established,^{8,9} reinforces the argument^{1,3} that Hauser-Feshbach calculations are a very promising spectroscopic tool. However, there are uncertainties in assigning spins via Hauser-Feshbach calculations demonstrated by examples in Fig. 5. Plotted in this figure are the $\frac{5}{2}^+$, $\frac{7}{2}^+$,

$\frac{9}{2}^+$, and $\frac{11}{2}^+$ members of the ground-state band. The curves are HF predictions for different spin-parities at a given excitation energy. For the known $\frac{5}{2}^+$, $\frac{7}{2}^+$, and $\frac{9}{2}^+$ states, the Hauser-Feshbach calculations with $J^\pi = \frac{5}{2}^-$, $\frac{7}{2}^-$, and $\frac{9}{2}^-$, respectively, are just as acceptable as those with the correct spin-parity. Hauser-Feshbach calculations with $J^\pi = \frac{9}{2}^+$ and $\frac{11}{2}^+$ will equally well fit the experimental angular distribution of the $\frac{11}{2}^+$, 5.536-MeV state. Nevertheless, the uncertainties just discussed may be removed if one is able to measure cross sections at 0° .

Figure 6 shows most of the high-spin states suggested by the present experiment. The HF curves are the closest ones to the experimental data and for many of these states only one or at most two curves fit the experimental angular distributions. Looking individually at each of the angular distributions we can suggest the best value for the spin of each state analyzed. Plotted on the left side of the figure are the states at

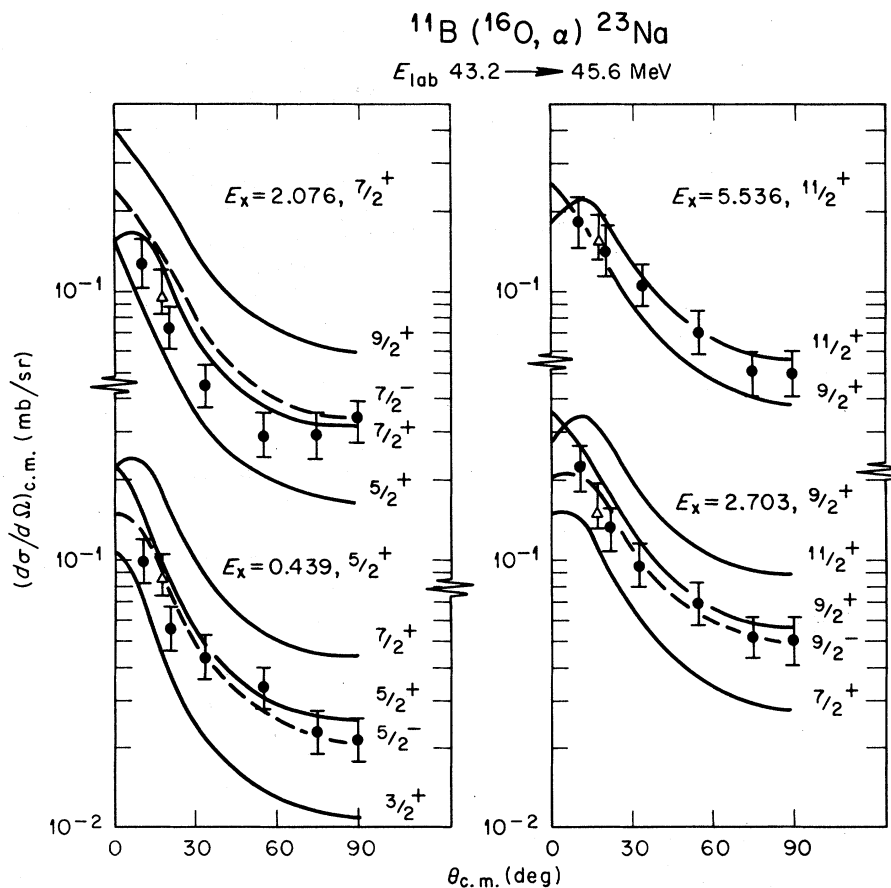


FIG. 5. Comparison of experimental angular distributions with different Hauser-Feshbach predictions for various spin-parities at a given excitation energy. The solid lines are predictions for positive-parity states, the dashed lines for negative-parity states. The states shown have spin-parities previously established (Refs. 8 and 9).

9.84, 11.28, 13.15, and 13.82 MeV. The state at 9.84 MeV has been suggested by Cormier *et al.*¹⁰ to be the $\frac{17}{2}^+$ member of the ground-state band. The basis for this assignment is the decay scheme observed in the population of this state by the $^{12}\text{C}(^{12}\text{C}, b\gamma)$ reaction. In Fig. 6 the angular distribution that best fits the experimental points is the $\frac{17}{2}^+$ curve. For this case the distinction between negative- and positive-parity states is more pronounced than for the low-spin states discussed previously.

The state at 11.28 MeV is very strongly excited in our spectrum (Fig. 1) but it is not observed in the work of Cormier *et al.*¹⁰ According to our

measured angular distribution this state is also a $\frac{17}{2}^+$.

The state at 13.14 MeV agrees with a $\frac{15}{2}^+$ or $\frac{15}{2}^-$ angular distribution and the one at 13.82 MeV agrees with a $\frac{17}{2}^+$. We suggest that these two states might be the $\frac{15}{2}^+$ and $\frac{17}{2}^+$ members of the $K = \frac{1}{2}^+$ rotational band.

The right side of Fig. 6 shows the states at 10.3, 10.9, 14.24, and 14.70 MeV. The state at 10.3 MeV is consistent with a $\frac{13}{2}^+$ or $\frac{13}{2}^-$. The energy is appropriate for this state to be the $\frac{13}{2}^-$ member of the $K = \frac{1}{2}^-$ band (see Sec. V). The state at 10.9 MeV agrees uniquely with a $\frac{13}{2}^+$ and we suggest that this can be a member of the $K = \frac{1}{2}^+$ band. Finally, the 14.24-MeV state agrees with a $\frac{17}{2}^+$ or $\frac{19}{2}^+$ angular distribution and the 14.70-MeV state agrees with a spin of $\frac{17}{2}^+$.

Column 4 of Table I shows the spin-parities selected by this method for the states from 0 to 15 MeV of excitation whose angular distributions and Hauser-Feshbach fits are shown on Figs. 3 and 4.

In the energy region from 5.74 to 9.04 MeV there were many states that were not resolved. The states at 5.74 and 5.77 MeV are an example. They were fitted either by a $\frac{5}{2}^+$ and $\frac{1}{2}^+$ or a $\frac{3}{2}^+$ and $\frac{3}{2}^+$ combination which is consistent with the spins suggested in Ref. 8. From 6.23 to 6.35 MeV there are four known states,⁸ two $\frac{1}{2}$ states which contribute little to the summed cross section, the 6.35-MeV $\frac{9}{2}^-$ member of the $K = \frac{1}{2}^-$ band⁹ and the 6.23-MeV state suggested to be the $\frac{13}{2}^+$ member^{9, 10} of the ground-state rotational band. The HF calculations best fit the data with a $\frac{9}{2}^+$ and $\frac{9}{2}^-$ combination (see Fig. 3) consistent with the spins of Ref. 8, but we think enough evidence exists to favor an assignment of $\frac{13}{2}^+$ for the 6.23-MeV state.^{9, 10} If this is so, the HF sum for $\frac{9}{2}^-$ and $\frac{13}{2}^+$ states predicts a cross section which exceeds the experimental data by a factor of 1.8. For the present experiment this is the only case for which the statistical model prediction is off by more than the experimental uncertainty ($\pm 20\%$).

Other unresolved states were at 6.57 and 6.73 MeV. We fitted these states with a $\frac{5}{2}^+$ and $\frac{3}{2}^+$ combination, which agrees with the spins suggested in Ref. 8. The states at 6.81 and 6.86 MeV can have the combination $\frac{5}{2}^+$ and $\frac{5}{2}^+$ or $\frac{3}{2}^+$ and $\frac{7}{2}^+$ according to the HF angular distribution, in agreement with previous suggestions to the 6.86-MeV state.⁸ From 7.07 to 7.156 MeV there are four known states⁸; spin-parities for three have been suggested as $\frac{5}{2}^-$, $\frac{3}{2}^-$, and $\frac{3}{2}^+$ or $\frac{5}{2}^+$. Our data are consistent with spins for the four states of either $\frac{5}{2}^+$, $\frac{3}{2}^-$, $\frac{5}{2}^+$, and $\frac{7}{2}^+$ or $\frac{5}{2}^+$, $\frac{3}{2}^-$, $\frac{3}{2}^+$, and $\frac{9}{2}^+$. For the states from 7.38 to 7.44 MeV the combination $\frac{3}{2}^-$, $\frac{9}{2}^+$, and $\frac{5}{2}^+$ seems to be the best fit to the

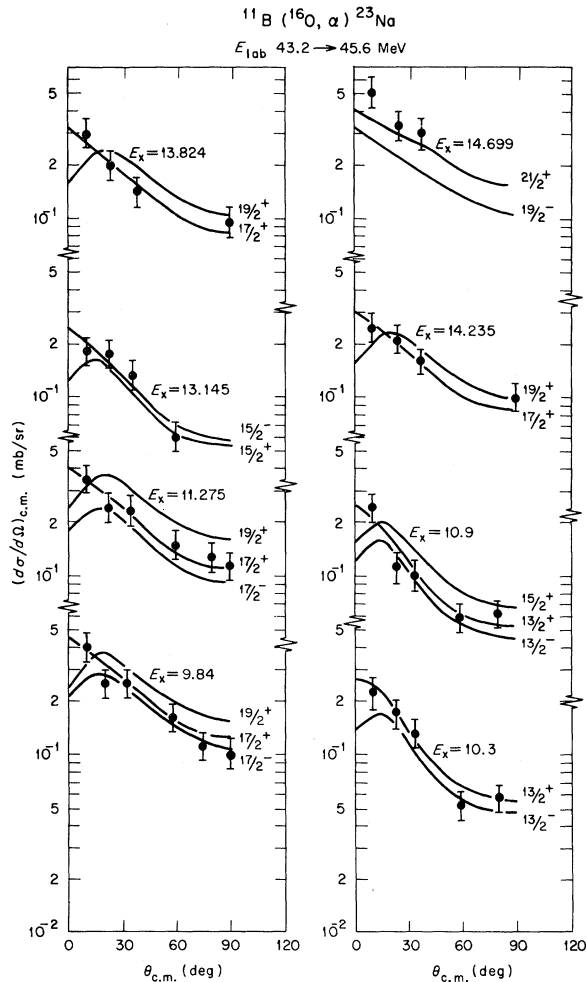


FIG. 6. Experimental angular distributions for the high-spin states compared to the different Hauser-Feshbach predictions. The states at 9.84 and 10.3 MeV have been previously suggested to have spin-parities of $\frac{17}{2}^+$ (Ref. 10) and $\frac{13}{2}^-$ (Ref. 9), respectively. The rest of the states are discussed in the text.

data, suggesting that the 7.41 MeV ($\frac{9}{2}^+$) state might be a member of the $K = \frac{1}{2}^+$ band; however, the combination $\frac{1}{2}^-$, $\frac{11}{2}^-$, and $\frac{3}{2}^+$ cannot be excluded. Of the unresolved states at 8.30, 8.32, and 8.36 MeV, the 8.30- and 8.36-MeV states were excited in ($^3\text{He}, d$) reactions¹⁹ with a probable $L=3$ transfer and thus have spin-parities of $\frac{7}{2}^-$ or $\frac{5}{2}^-$. Using this suggestion we obtain three possible combinations: three $\frac{7}{2}^-$'s; $\frac{7}{2}^-$, $\frac{9}{2}^-$, and $\frac{5}{2}^-$; and two $\frac{5}{2}^-$'s and one $\frac{11}{2}^-$. The states excited from 8.46 to 8.6 MeV were not analyzed, since previous information on some of the spin values is not available. Near 9 MeV of excitation there are two states separated by 100 keV: 8.94 and 9.04. Both are also excited in the $^{12}\text{C}(^{12}\text{C}, p)$ reaction.⁹ The 9.04-MeV state has been suggested^{9, 10} as the $\frac{15}{2}^+$ member of the ground-state rotational band. We fitted the sum of these two states with the combinations $\frac{15}{2}^+$ and $\frac{11}{2}^+$; possibly the $\frac{11}{2}^+$ state is a member of the $K = \frac{1}{2}^+$ band.

V. DISCUSSION OF THE STRUCTURE IN ^{23}Na

A. Nilsson-model calculations

According to Nilsson-model calculations⁹ there are several rotational bands in ^{23}Na . The ground-state band with the Nilsson configuration $\frac{3}{2}^+(211)$ has been observed by several authors^{8, 19} for the low-spin members and by Frank *et al.*⁹ and Cormier *et al.*¹⁰ up to the $\frac{15}{2}^+$ and $\frac{17}{2}^+$ states, respectively. In this work we confirmed the previous suggestions and proposed that the 14.24- and 14.70-

MeV states are the $\frac{19}{2}^+$ and $\frac{21}{2}^+$ members. It is very interesting to note that the structure of the ground-state rotational band for ^{23}Mg proposed by Sperr *et al.*²⁰ agrees within 100 keV with the energies of the states we are suggesting for ^{23}Na up to the $\frac{21}{2}^+$ state.

A second rotational band with Nilsson configuration $\frac{1}{2}^+(211)$ has been predicted and identified,^{9, 19} starting with the 2.39-MeV $\frac{1}{2}^+$ state. Previous suggestions have been made for members of this band up to the $\frac{7}{2}^+$ state. With this experiment we propose states in this band up to the $\frac{17}{2}^+$ member. These are (E in MeV, J^π): 7.41, $\frac{9}{2}^+$; 8.94, $\frac{11}{2}^+$; 10.9, $\frac{13}{2}^+$; 13.15, $\frac{15}{2}^+$; and 13.82, $\frac{17}{2}^+$. Existing Nilsson-model calculations⁹ place the $\frac{9}{2}^+$ and $\frac{11}{2}^+$ states at 7.37 and 8.99 MeV, respectively, in excellent agreement with the experimental suggestions.

With the Nilsson configuration $\frac{1}{2}^-(101)$ begins the first negative-parity band. This band has been observed up to the $\frac{13}{2}^-$ member.⁹ In this work we confirm the previously suggested assignments, particularly for the 6.04-MeV, $\frac{7}{2}^-$ and 10.3-MeV, $\frac{13}{2}^-$ states. Further, we suggest that the 11.58-MeV state be considered a good candidate for the $\frac{15}{2}^-$ member. We do not have a suggestion for the $\frac{11}{2}^-$ state, since in the energy region where we expect to find it⁹ we have lost the needed information because of the previously mentioned carbon contamination problem. We recognize that this problem may lead to faulty association of higher-spin states to the excited bands, because of the

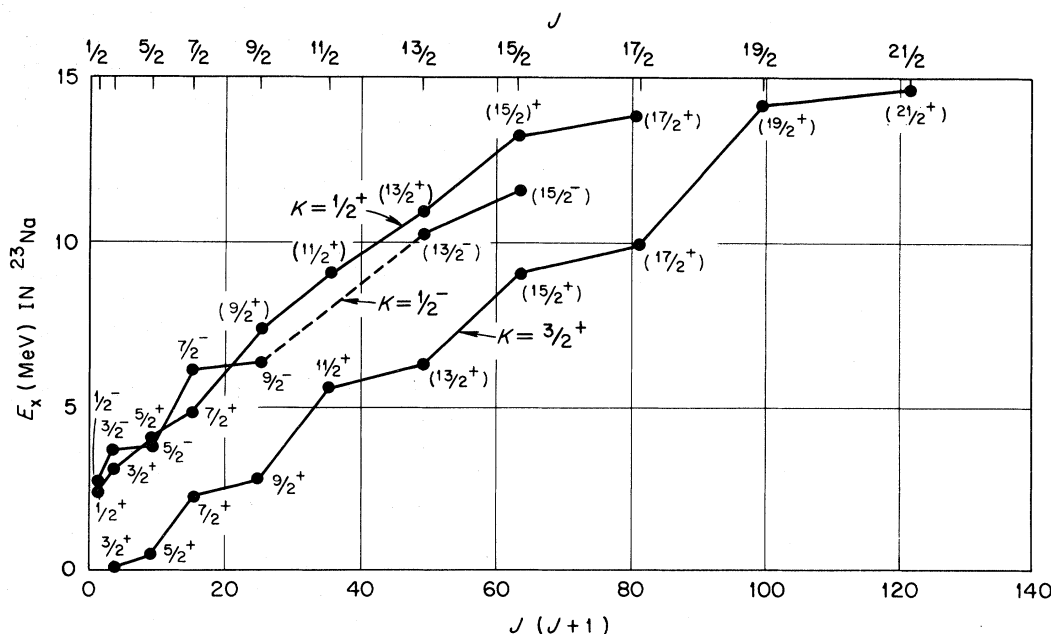


FIG. 7. A plot of the $K = \frac{3}{2}^+$, $T = \frac{1}{2}$; $K = \frac{1}{2}^+$, $T = \frac{1}{2}$; and $K = \frac{1}{2}^-$, $T = \frac{1}{2}$ rotational bands in ^{23}Na .

chance that we might miss states which occur at lower excitation; however, we show in Fig. 7 our suggestions for the $T = \frac{1}{2}$ bands with $K^\pi = \frac{3}{2}^+$, $\frac{1}{2}^+$, and $\frac{1}{2}^-$.

B. Shell-model calculations

There is obviously one annoying feature insofar as making a simple rotational model analysis of the observed spectrum is concerned. That is the existence of a $J^\pi = \frac{17}{2}^+$ state at 11.28 MeV. This state occurs between the proposed $\frac{17}{2}^+$ members of the ground-state and first-excited-state bands. We have made conventional shell-model calculations of the excitation spectrum of high-spin states in ^{23}Na , and, as we shall now discuss, they indicate that it may be difficult to make a simple rotational model analysis of the high-spin states.

Let us first describe the shell-model calculation. An inert ^{16}O core is assumed, and all possible states of Pauli-allowed configurations of particles in the $(sd)^7$ shell are included in the model space. We assume an effective residual interaction consisting of only one- and two-particle interactions. The matrix elements of the one-body operator are deduced from the observed spectrum of ^{17}O and ^{17}F . For the matrix elements of the two-body interaction we use those published by Preedom and Wildenthal.²⁴ A model completely analogous to this one was extremely successful in describing the observed spectrum of high-spin states in ^{22}Na (Ref. 25). The model not only reproduced the collective rotational structure of these states, but it reproduced in quantitative fashion the significant deviations on this structure from the simple rotational picture.

In Fig. 8, the excitation spectrum of states with $J^\pi \geq \frac{13}{2}^+$ as calculated in this model for ^{23}Na is compared with the observed spectrum. For comparison purposes, we assumed that the lowest states for each spin in the calculated and observed spectrum are members of the ground-state band. With this assumption the observed energies of the $J^\pi = \frac{13}{2}^+$ and $\frac{15}{2}^+$ states are accurately reproduced in the calculated spectrum. However, there is significant discrepancy for the $J^\pi = \frac{17}{2}^+$ state. It is 1 MeV below the lowest $J^\pi = \frac{17}{2}^+$ state in the calculated spectrum. There are two, almost degenerate, $\frac{17}{2}^+$ states in the calculated spectrum around 11 MeV. One of these is the 11.28-MeV state which is unaccounted for in the rotational model description discussed above. Thus, the shell-model accurately predicts the existence of the extra state, but it apparently underestimates the mixing of these two states. There is also a 1-MeV discrepancy between the observed and calculated positions of the $J^\pi = \frac{19}{2}^+$ state and a 2-MeV

discrepancy between the $\frac{21}{2}^+$ states. These discrepancies are distinctly greater than was the case for the ground-state band in ^{22}Na .

Perhaps of more interest is the calculation for states outside the ground-state band. One would have an extremely difficult job interpreting the shell-model spectrum of states outside the ground-state band in terms of any simple rotational model. There appears to be many extra high-spin states. One would have to consider the existence of at least three bands, and introduce significant degrees of band mixing. Insofar as a theory-experiment comparison is concerned, there are complications. We have discussed the fact that it is impossible to make a complete analysis of the observed spectra because of target ^{12}C -contamination problems and because of the existence of several unresolvable states. It is in almost exactly those regions where there are such problems that the shell-model predicts extra states that do not fit into any rotational model. In addition, there is the fact that in calculations of the low-spin states in ^{23}Na in this same model, the calculated positions of states in the first-excited positive-parity rotational band are low by about 0.5 MeV. This suggests that the observed high-spin states for this band may be significantly higher in energy than their calculated positions. All these com-

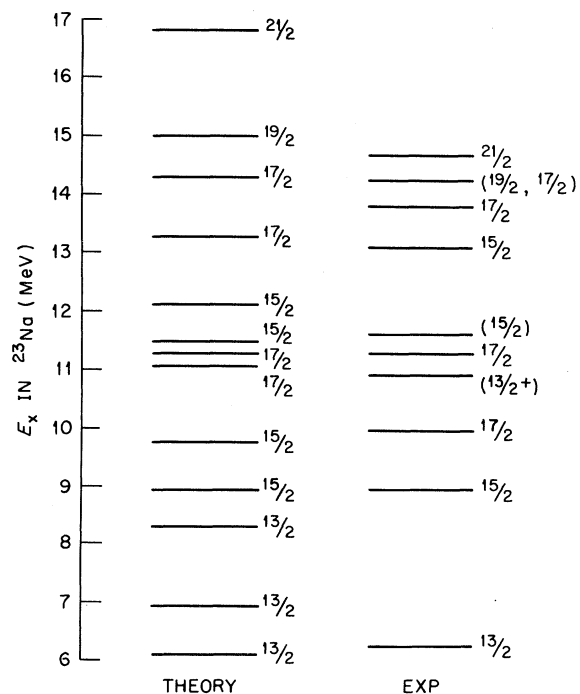


FIG. 8. Comparison of the high-spin states observed with predictions of shell-model theory discussed in the text.

plications make necessary more experimental information in order to decide whether or not the "extra" high-spin states predicted by this shell-model calculation are present.

VI. SUMMARY

The excellent agreement found between the experimental and HF angular distributions for most of the states in ^{23}Na whose spins and parities have been previously established, strongly supports the statistical-model description for the reaction mechanism. There is only one exception to the general agreement, namely, the $\frac{13}{2}^+$ state at 6.23 MeV, whose calculated angular distribution exceeds the experimental cross section by 80%. The fact that for this and other reactions^{1,7} some deviations are found from the general statistical behavior is indicative that for these cases a more complex mechanism is occurring. However, most evidence indicates that comparison of the experimental results to model predictions allows spin assignments to within one unit of angular momenta provided that fluctuation phenomena have

been properly taken into account.

Candidates of the $K = \frac{1}{2}^+$, $\frac{1}{2}^-$, and $\frac{3}{2}^+$ (ground state) Nilsson bands with spins up to $\frac{17}{2}^+$, $\frac{15}{2}^-$, and $\frac{21}{2}^+$, respectively, have been proposed. Angular differential cross sections for these states are consistent with Hauser-Feshbach calculations. Shell-model calculations were performed and were found to roughly reproduce the structure of the excitation spectrum of high-spin states in the ground-state rotational band. However, these calculations suggest that the simple rotational picture breaks down for high-spin states outside the ground-state band, particularly if one considers that this picture cannot account for the second $\frac{17}{2}^+$ state observed at 11.27 MeV.

ACKNOWLEDGMENTS

Valuable discussions with Dr. D. Evers, Dr. R. S. Malmin, and Dr. H. V. Klapdor, concerning the data and analysis are gratefully acknowledged. One of us (JGC) wants to express his gratitude to the Oak Ridge National Laboratory for the financial support that made possible his participation in this study.

*Research participation sponsored by Oak Ridge National Laboratory.

†Research participation sponsored in part by Oak Ridge National Laboratory.

‡Operated by Union Carbide Corporation for the U. S. Atomic Energy Commission.

¹J. Gomez del Campo, J. L. C. Ford, Jr., R. L. Robinson, P. H. Stelson, and S. T. Thornton, Phys. Rev. C **9**, 1258 (1974).

²D. L. Hanson, R. G. Stokstad, K. A. Erb, C. Olmer, and D. A. Bromley, Phys. Rev. C **9**, 929 (1974).

³H. V. Klapdor and H. Reiss, Z. Phys. **262**, 83 (1973).

⁴L. R. Greenwood, K. Katori, R. E. Malmin, T. H. Braid, J. C. Stoltzfus, and R. H. Siemssen, Phys. Rev. C **6**, 2112 (1972).

⁵J. L. C. Ford, Jr., J. Gomez del Campo, R. L. Robinson, P. H. Stelson, and S. T. Thornton, Z. Phys. **269**, 147 (1974).

⁶R. G. Stokstad, in *Proceedings of the International Conference on Reactions between Complex Nuclei, Nashville, Tennessee, 10-14 June 1974*, edited by R. L. Robinson, F. K. McGowan, J. B. Ball, and J. H. Hamilton (North-Holland, Amsterdam/American Elsevier, New York, 1974), Vol. 2, p. 327.

⁷L. K. Fifield, R. W. Zurmühle, and D. P. Balamuth, Phys. Rev. C **8**, 2217 (1973).

⁸P. M. Endt and C. Van der Leun, Nucl. Phys. **A214**, 1 (1973).

⁹G. C. Frank, R. V. Elliot, R. H. Spear, and J. A. Kuehner, Can. J. Phys. **51**, 1155 (1973).

¹⁰T. M. Cormier, E. R. Cosman, L. Grodzins, O. Hansen, S. Steadman, K. Van Bibber, and G. Young, in *Proceedings of the International Conference on*

Reactions between Complex Nuclei, Nashville, Tennessee, 10-14 June 1974 (see Ref. 6), Vol. 1, p. 172.

¹¹T. Ericson, Phys. Rev. Lett. **5**, 430 (1960).

¹²D. M. Brink and R. O. Stephen, Phys. Lett. **5**, 77 (1963).

¹³S. K. Penny (private communication).

¹⁴E. Almqvist, J. A. Kuehner, D. McPherson, and E. W. Vogt, Phys. Rev. **136**, B84 (1964).

¹⁵A. Gilbert and A. G. W. Cameron, Can. J. Phys. **43**, 1446 (1965).

¹⁶V. Facchini and E. Saetta-Menichella, Energ. Nucl. (Milan) **15**, 54 (1968).

¹⁷U. C. Schlotthauer-Voos, H. G. Bohlen, W. Von Oertzen, and R. Bock, Nucl. Phys. **A180**, 385 (1972).

¹⁸R. E. Malmin, Ph.D. thesis, Indiana University, 1972 (unpublished).

¹⁹J. R. Powers, H. T. Fortune, R. Middleton, and O. Hansen, Phys. Rev. C **4**, 2030 (1971).

²⁰P. Sperr, D. Evers, K. Rudolph, W. Assmann, E. Spindler, P. Konrad, and G. Denhöfer, Phys. Lett. **49B**, 345 (1974).

²¹L. McFadden and G. R. Satchler, Nucl. Phys. **84**, 177 (1966).

²²C. M. Perey and F. G. Perey, Nucl. Data **B10**, 539 (1972).

²³A. J. Buffa, Jr., and M. K. Brussel, Nucl. Phys. **A195**, 545 (1972).

²⁴B. M. Freedom and B. H. Wildenthal, Phys. Rev. C **7**, 1633 (1972).

²⁵J. Gomez del Campo, J. L. C. Ford, Jr., R. L. Robinson, P. H. Stelson, J. B. McGrory, and S. T. Thornton, Phys. Lett. **46B**, 180 (1973).